

## The Phase Transitions of 1,4-Dialkyl-1,4-diazoniabicyclo[2.2.2]octane Bis(tetrafluoroborate), $C_n$ -DABCO- $C_n$ -( $BF_4$ )<sub>2</sub> ( $10 \leq n \leq 22$ )

Tohru TERADA, Takashi NOGAMI,\* and Yasuhiko SHIROTA  
 Department of Applied Chemistry, Faculty of Engineering, Osaka University,  
 Yamadaoka, Suita, Osaka 565  
 (Received May 27, 1988)

The phase transitions of a series of title compounds were investigated by means of DSC, IR absorption spectra, and measurements of ionic conductivities. All of the compounds exhibited phase transitions in the range of 77–110 °C. The IR absorption spectra clarified that conformational change in the alkyl chain occurred above the transition temperature. The temperature dependences of the ionic conductivities of  $BF_4^-$  showed conductivity jumps by a factor of 9–120 around the transition temperatures. A comparison of the DSC results and the ionic conductivities of  $BF_4^-$ -salts with those of the corresponding Br-salts showed that the former compounds have higher transition temperatures, smaller transition enthalpies (and, accordingly, smaller transition entropies), and smaller values of the conductivity jumps than the latter. These results show that  $BF_4^-$ -salts are more rigid than Br-salts in the low temperature phase and that the motion of the alkyl group of the former salts is less vigorous than the latter in the high-temperature phase. By observing the crystal with a polarization microscope under crossed Nicols condition, it was found that optical anisotropy was diminished gradually with the elevation of the temperature and disappeared completely above  $T_c$  without changing the crystal shape.

The phase transitions of various types of quaternary alkyl halide salts of 1,4-diazabicyclo[2.2.2]octane (DABCO) have been studied by means of measurements of the ionic conductivities of the halide anion, DSC, IR, and Raman spectroscopies.<sup>1–7</sup> Conductivity jumps of the halide anion by from two to three orders of magnitude were observed around the transition temperatures. The IR and Raman spectroscopies of the salts established that transitions are induced by the vigorous motion of the alkyl chain, accompanied with its conformational change.<sup>8</sup> Some of the unsymmetric bis(quaternary alkyl bromide) salts of DABCO gave a metastable state after having been heated above the transition temperature and then cooled.<sup>4,5</sup> The study of molecular motion in a solid is important as a model system for the melting of materials and the glass transition of polymers, etc. As an extension of the previous studies, we have investigated the phase transition of a series of symmetric bis(quaternary salts) of DABCO possessing the tetrafluoroborate anion. We adopted DABCO- $BF_4$  salts to see the effect of the different type of anion from the previous ones (spherical and monoatomic halide anion → tetrahedral and pentaatomic  $BF_4^-$ ) on the phase transitions. The materials in this study will be abbreviated by the number of alkyl carbons. For example, 1,4-didodecyl-1,4-diazoniabicyclo[2.2.2]octane bis(tetrafluoroborate) is abbreviated to  $C_{12}$ -DABCO- $C_{12}$ -( $BF_4$ )<sub>2</sub>. Thus, the materials in this study will generally be abbreviated as  $C_n$ -DABCO- $C_n$ -( $BF_4$ )<sub>2</sub>.

### Experimental

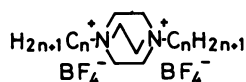
**Materials.** All of the materials were synthesized by treating the corresponding  $C_n$ -DABCO- $C_n$ -Br<sub>2</sub><sup>1,2</sup> with tetrafluoroboric acid. Table 1 summarizes the reaction media and precipitation media of  $C_n$ -DABCO- $C_n$ -Br<sub>2</sub> and  $C_n$ -DABCO- $C_n$ -( $BF_4$ )<sub>2</sub> ( $1 \leq n \leq 22$ ), the solvents of recrystallization, and the yields of  $C_n$ -DABCO- $C_n$ -( $BF_4$ )<sub>2</sub> after one recrystallization.  $C_n$ -DABCO- $C_n$ -Br<sub>2</sub> ( $1 \leq n \leq 9$ ) could not be purified by recrystallization because of their hygroscopic properties; therefore, they were directly used, without recrystallization, for the synthesis of tetrafluoroborate.<sup>9</sup> A protonated salt, H-DABCO-H-( $BF_4$ )<sub>2</sub>, was synthesized by the reaction of DABCO with tetrafluoroboric acid in ethyl alcohol; it is denoted as  $n=0$  in Table 1.  $C_n$ -DABCO- $C_n$ -( $BF_4$ )<sub>2</sub> ( $1 \leq n \leq 9$ ) and H-DABCO-H-( $BF_4$ )<sub>2</sub> were recrystallized five times, and  $C_n$ -DABCO- $C_n$ -( $BF_4$ )<sub>2</sub> ( $10 \leq n \leq 22$ ), three times, before the measurements. Most of the analytical data of  $C_n$ -DABCO- $C_n$ -( $BF_4$ )<sub>2</sub> ( $10 \leq n \leq 22$ ) were satisfactory.<sup>10</sup> All of the materials decomposed above 300 °C without melting.

The synthetic method will be described for  $C_{16}$ -DABCO- $C_{16}$ -( $BF_4$ )<sub>2</sub> as typical. The reaction was conducted in a Teflon beaker.  $C_{16}$ -DABCO- $C_{16}$ -Br<sub>2</sub> (0.723 g, 1 mmol) was dissolved into ethyl alcohol (20 ml), and then two molar amounts of tetrafluoroboric acid (42%) was stirred in. The homogeneous solution was then stirred into benzene (180 ml), and the mixture was cooled by ice in order to precipitate the product. The white precipitate was collected, dried in a vacuum, and recrystallized three times from ethyl alcohol.

**Measurements.** The ionic conductivities, DSC, and IR absorption spectra were measured by methods reported previously.<sup>1,2</sup>

### Results and Discussion

**DSC Measurements.** The DSC measurements were made with a scan speed of 5 °C min<sup>-1</sup>.  $C_n$ -DABCO- $C_n$ -( $BF_4$ )<sub>2</sub> ( $10 \leq n \leq 22$ ) exhibited a single endothermic signal in the range of 77–110 °C. When they were



$C_n$ -DABCO- $C_n$ -( $BF_4$ )<sub>2</sub>

Table 1. Reaction and Precipitation Media,<sup>a)</sup> Solvents of Recrystallization,<sup>a)</sup> and Yields

| <i>n</i> | <i>C<sub>n</sub></i> -DABCO- <i>C<sub>n</sub></i> -Br <sub>2</sub> |                              | <i>C<sub>n</sub></i> -DABCO- <i>C<sub>n</sub></i> -(BF <sub>4</sub> ) <sub>2</sub> |                              | Yield <sup>d)</sup><br>% |
|----------|--|------------------------------|--|------------------------------|--------------------------|
|          | Reaction/precipitation media                                       | Solvent of recrystallization | Reaction/precipitation media   | Solvent of recrystallization |                          |
| 0        | —  | —                            | EtOH/EtOH <sup>c)</sup>  | EtOH-H <sub>2</sub> O        | 22.9                     |
| 1        | MeOH   | b)                           | EtOH/EtOH <sup>c)</sup>  | EtOH-H <sub>2</sub> O        | 43.2                     |
| 2        | MeOH   | b)                           | EtOH/EtOH <sup>c)</sup>  | EtOH-H <sub>2</sub> O        | 64.2                     |
| 3        | MeOH   | b)                           | EtOH/EtOH <sup>c)</sup>  | EtOH-H <sub>2</sub> O        | 21.1                     |
| 4        | MeOH   | b)                           | EtOH/EtOH <sup>c)</sup>  | EtOH-H <sub>2</sub> O        | 29.3                     |
| 5        | MeOH   | b)                           | EtOH/EtOH <sup>c)</sup>  | EtOH-H <sub>2</sub> O        | 40.0                     |
| 6        | MeOH   | b)                           | EtOH/EtOH <sup>c)</sup>  | EtOH-H <sub>2</sub> O        | 4.8                      |
| 7        | MeOH   | b)                           | EtOH/EtOH <sup>c)</sup>  | EtOH-H <sub>2</sub> O        | 21.1                     |
| 8        | MeOH   | b)                           | EtOH/Bz  | EtOH-H <sub>2</sub> O        | 16.5                     |
| 9        | MeOH   | b)                           | EtOH/Bz  | EtOH-H <sub>2</sub> O        | 6.3                      |
| 10       | MeOH/Bz  | MeCN                         | EtOH/EtOH <sup>c)</sup>  | MeOH-Bz                      | 40.0                     |
| 11       | MeOH/Ether   | MeCN                         | EtOH/H <sub>2</sub> O  | MeOH-Bz                      | 37.1                     |
| 12       | MeOH/Bz  | MeCN                         | EtOH/H <sub>2</sub> O  | MeOH-Bz                      | 43.2                     |
| 13       | MeOH/Ether   | MeCN                         | MeOH/Bz  | MeOH                         | 65.8                     |
| 14       | MeOH/Bz  | MeCN                         | MeOH/Bz  | EtOH                         | 86.4                     |
| 15       | MeOH/Ether   | EtOH                         | MeOH/Bz  | MeOH                         | 82.4                     |
| 16       | MeOH/Bz  | EtOH                         | EtOH/Bz  | EtOH                         | 82.3                     |
| 17       | MeOH/Bz  | EtOH                         | MeOH/Bz  | EtOH                         | 86.2                     |
| 18       | MeOH/Bz  | EtOH                         | EtOH/Bz  | EtOH                         | 74.5                     |
| 22       | MeOH/Bz  | EtOH                         | EtOH/Bz  | EtOH                         | 78.2                     |

a) MeOH=methyl alcohol, Bz=benzene, Ether=diethyl ether, MeCN=acetonitrile, EtOH=ethyl alcohol. b) Purification by recrystallization could not be done because of the hygroscopic property. c) The ethanol solution of the reaction was poured into a large amount of ethanol cooled by ice. d) Yields after one recrystallization.

Table 2. Transition Temperatures (*T<sub>c</sub>*), Transition Enthalpies ( $\Delta H$ ), Transition Entropies ( $\Delta S$ ), and Ratios of the Ionic Conductivities below ( $\sigma_1$ ) and above ( $\sigma_h$ ) the Transition Temperature of *C<sub>n</sub>*-DABCO-*C<sub>n</sub>*-(BF<sub>4</sub>)<sub>2</sub>

| <i>n</i> | <i>T<sub>c</sub></i><br>°C | $\Delta H$<br>kJ mol <sup>-1</sup> | $\Delta S$<br>J mol <sup>-1</sup> deg <sup>-1</sup> | $\sigma_h/\sigma_1$ <sup>a)</sup> |
|----------|----------------------------|------------------------------------|---|-----------------------------------|
| 10       | 77                         | 20.1                               | 58  | — (850)                           |
| 11       | 84                         | 23.7                               | 66  | 14 (630)                          |
| 12       | 89                         | 40.5                               | 112   | 42 (920)                          |
| 13       | 95                         | 34.8                               | 94  | 13 (1500)                         |
| 14       | 96                         | 55.8                               | 151   | 15 (1400)                         |
| 15       | 99                         | 42.7                               | 115   | 47 (980)                          |
| 16       | 102                        | 67.8                               | 181   | 20 (1200)                         |
| 17       | 101                        | 41.5                               | 111   | 24 (3600)                         |
| 18       | 106                        | 74.1                               | 196   | 120 (1400)                        |
| 22       | 110                        | 105.6                              | 276   | 9 (2200)                          |

a) The values in parentheses indicate  $\sigma_h/\sigma_1$  values observed for *C<sub>n</sub>*-DABCO-*C<sub>n</sub>*-Br<sub>2</sub> (after Ref. 2).

cooled after having been heated above the transition temperature, they showed exothermic signals around the transition temperature. The values of the endothermic and exothermic heats of transition were almost equal, within the limits of experimental error. Thus, the phase transition is almost reversible. Part of Table 2 summarizes the transition temperatures, transition enthalpies, and transition entropies. The DSC signals expected for *C<sub>n</sub>*-DABCO-*C<sub>n</sub>*-(BF<sub>4</sub>)<sub>2</sub> (1≤*n*≤9) were below the limit of sensitivity of the DSC apparatus. Figure 1 plots the transition temperatures (*T<sub>c</sub>*) of *C<sub>n</sub>*-DABCO-*C<sub>n</sub>*-(BF<sub>4</sub>)<sub>2</sub> (10≤*n*≤22) against the

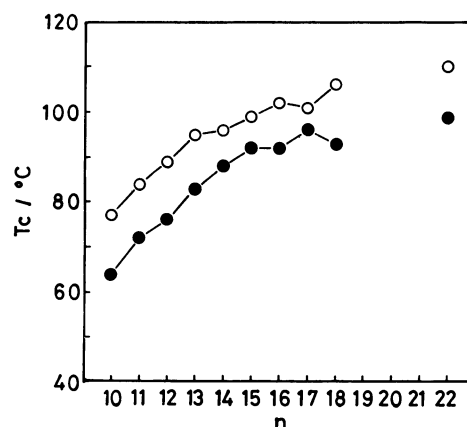


Fig. 1. The plot of the transition temperatures (*T<sub>c</sub>*) against the carbon number of alkyl group (*n*) of *C<sub>n</sub>*-DABCO-*C<sub>n</sub>*-(BF<sub>4</sub>)<sub>2</sub>. The *T<sub>c</sub>*-*n* plot of *C<sub>n</sub>*-DABCO-*C<sub>n</sub>*-Br<sub>2</sub> are also shown for the sake of comparison. ○ *C<sub>n</sub>*-DABCO-*C<sub>n</sub>*-(BF<sub>4</sub>)<sub>2</sub>, ● *C<sub>n</sub>*-DABCO-*C<sub>n</sub>*-Br<sub>2</sub>.

carbon number (*n*) of the alkyl group. *T<sub>c</sub>* was obtained by the onset of the endothermic signal. This figure also shows the *T<sub>c</sub>*-*n* plot of *C<sub>n</sub>*-DABCO-*C<sub>n</sub>*-Br<sub>2</sub> (10≤*n*≤22)<sup>2)</sup> for the sake of comparison. *T<sub>c</sub>* tends to increase with the increase in the carbon number of the alkyl group. As will be described below, the phase transition is induced by the vigorous motion of the alkyl chain above *T<sub>c</sub>*. The increase in *T<sub>c</sub>* with the increase in *n* is caused by the fact that the van der Waals force between alkyl groups of the neighboring molecules becomes larger as *n* increases, while the

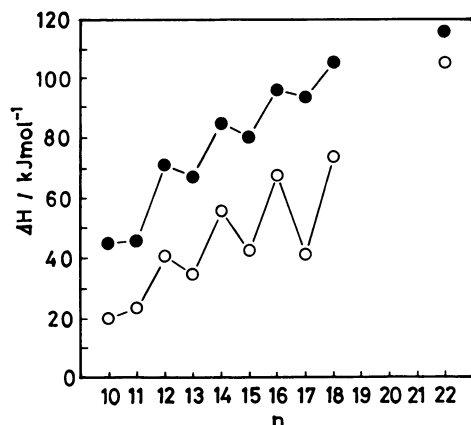


Fig. 2. The plot of the transition enthalpies ( $\Delta H$ ) against the carbon number of alkyl group ( $n$ ) of  $C_n$ -DABCO- $C_n$ -(BF<sub>4</sub>)<sub>2</sub>. The  $\Delta H$ - $n$  plot of  $C_n$ -DABCO- $C_n$ -Br<sub>2</sub> are also shown for the sake of comparison. ○  $C_n$ -DABCO- $C_n$ -(BF<sub>4</sub>)<sub>2</sub>, ●  $C_n$ -DABCO- $C_n$ -Br<sub>2</sub>.

onset temperature of the motion of alkyl chain shifts to the higher temperature range with this increase. The transition temperatures of BF<sub>4</sub>-salts were higher than those of the corresponding Br-salts. Thus, the former salts are harder than the latter in the low temperature phase. Figure 2 plots the transition enthalpies ( $\Delta H$ ) of  $C_n$ -DABCO- $C_n$ -(BF<sub>4</sub>)<sub>2</sub> ( $10 \leq n \leq 22$ ) against the carbon number of the alkyl group ( $n$ ). This figure also shows the  $\Delta H$ - $n$  plot of  $C_n$ -DABCO- $C_n$ -Br<sub>2</sub> for the sake of comparison. The  $\Delta H$  values of BF<sub>4</sub>-salts were smaller than those of the corresponding Br-salts. The even-odd number effect of alkyl carbon on  $\Delta H$  was clearly seen for BF<sub>4</sub>-salts as well as Br-salts, and this effect became larger with the increase in  $n$  in BF<sub>4</sub>-salts. It is well known that the melting points of normal alkanes show such an even-odd number effect. Accordingly, the distinct even-odd number effect shown in Fig. 2 suggests that the alkyl group of DABCO-salt plays an important role in the phase transitions. The plot of the transition entropies ( $\Delta S$ ) against the carbon number of the alkyl group (not shown here) also showed an even-odd number effect similar to that in Fig. 2. The  $\Delta S$  values of the BF<sub>4</sub>-salts were likewise smaller than those of the Br-salts; this suggests that the motion of the alkyl group of the former salts is less vigorous than that of the latter in the high-temperature phase.

**IR Absorption Spectroscopy.** The temperature dependence of the IR-absorption spectra of C<sub>17</sub>-DABCO-C<sub>17</sub>-(BF<sub>4</sub>)<sub>2</sub> was measured by means of the KBr method in order to gain more detailed information on the phase transitions. Figure 3 shows the IR spectra measured below and above the transition temperature (12 and 115 °C). The strong absorption around 1000–1150 cm<sup>-1</sup> is ascribable to BF<sub>4</sub><sup>-</sup>. The spectrum at 12 °C (Fig. 3(a)) exhibits fine structures (shown by the arrows). These structures are assigned to band

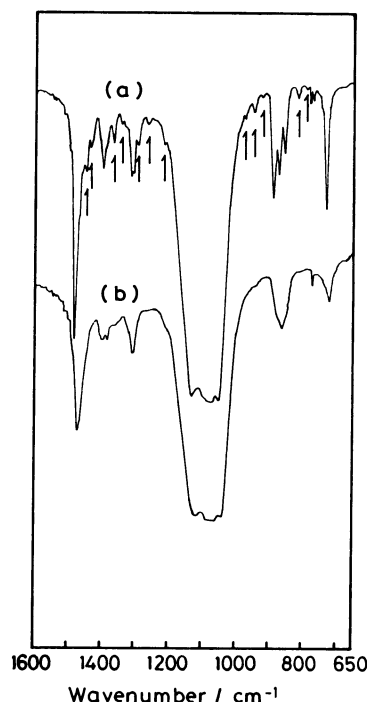


Fig. 3. IR absorption spectra of C<sub>17</sub>-DABCO-C<sub>17</sub>-(BF<sub>4</sub>)<sub>2</sub>. (a) 12 °C, (b) 115 °C.

progressions of the alkyl chain<sup>2)</sup> and are indicative of the trans-zigzag conformation of the alkyl chain in the low-temperature phase. Although a slight broadening was found, these band progressions were always observed with an elevation of the temperature up to the transition temperature. However, they disappeared suddenly around the transition temperature to give the structureless spectra shown in Fig. 3(b). The disappearance of the band progressions in the high-temperature phase indicates the conformational change in the alkyl chain induced by its vigorous motion in the solid.<sup>2)</sup> Thus, the phase transitions of the present materials were attributable to be the same origin as  $C_n$ -DABCO- $C_n$ -X<sub>2</sub> (X=Cl, Br, I).<sup>1-7)</sup>

**Ionic Conductivities.** In the measurements of ionic conductivities, the charge carrier was usually determined by applying a DC voltage to the sample, while injecting the common carrier ion into the sample.<sup>1,2)</sup> This was accomplished by mixing the authentic ionic conductor with the electrode material (graphite in many cases). Since the carrier concentration is maintained in such an experiment, the resistance of the sample does not change.<sup>1)</sup> Unfortunately, since no BF<sub>4</sub><sup>-</sup> conductor was reported, the above DC experiment could not be made for the present materials. By analogy with previous studies,<sup>1-7)</sup>  $C_n$ -DABCO- $C_n$ -(BF<sub>4</sub>)<sub>2</sub> is assumed to be the BF<sub>4</sub><sup>-</sup> conductor. This assumption is plausible because, although the two candidates for the charge carrier<sup>1)</sup> are quaternary DABCO cation and BF<sub>4</sub><sup>-</sup>, the quaternary DABCO

cation is too big to transport in the solid. On the other hand,  $\text{BF}_4^-$  is much smaller than the quaternary DABCO cation, and can transport in the solid. In other words, if the quaternary DABCO cation, which occupies most of the volume of the material, could move in the solid, the materials would not remain solid, but would be converted into liquid, especially above  $T_c$ .

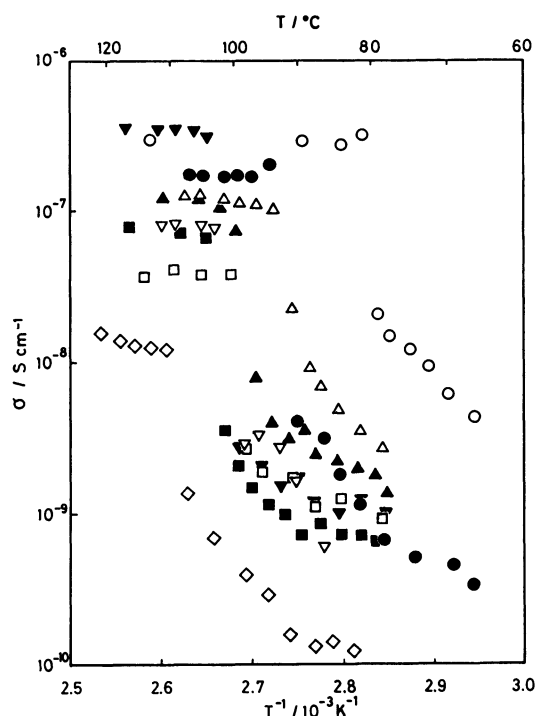
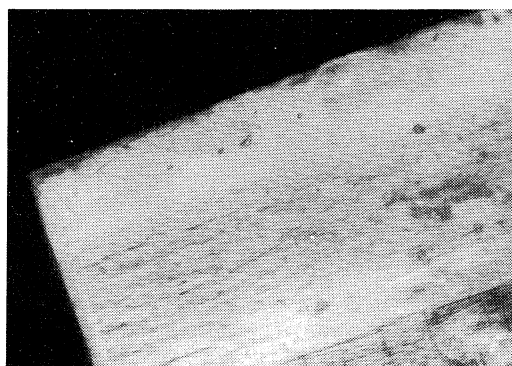
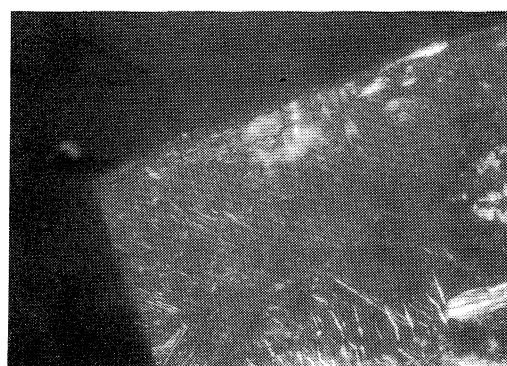


Fig. 4. Temperature dependence of the ionic conductivities of  $C_n\text{-DABCO-}C_n\text{-(BF}_4)_2$ .  
 $\bigcirc n=11$ ,  $\bullet n=12$ ,  $\triangle n=13$ ,  $\blacktriangle n=14$ ,  $\square n=15$ ,  $\blacksquare n=16$ ,  
 $\nabla n=17$ ,  $\blacktriangledown n=18$ ,  $\diamond n=22$ .

The ionic conductivities were measured for compressed pellet samples by the AC method.<sup>1,2)</sup> The temperature dependences of the ionic conductivities of  $C_n\text{-DABCO-}C_n\text{-(BF}_4)_2$  are shown in Fig. 4. Conductivity jumps were observed within the temperature width of 1.7–5.7 °C<sup>12)</sup> around the transition temperature<sup>13)</sup> for all of the materials. Part of Table 2 summarizes the ratios of the ionic conductivities below ( $\sigma_l$ ) and above ( $\sigma_h$ ) the conductivity jumps. This table also shows the values of  $\sigma_h/\sigma_l$  in  $C_n\text{-DABCO-}C_n\text{-Br}_2$  in parentheses for the sake of comparison. The  $\sigma_h/\sigma_l$  values of the  $\text{BF}_4^-$ -salts were found to be in the range of 9–120, whereas those of Br-salts were in the range of 850–3600.<sup>2)</sup> Thus, the conductivity jumps of  $\text{BF}_4^-$ -salts were much smaller than those of Br-salts. This can be explained by the following reasons. The conductivity jumps proved to arise from the formation of voids (conduction channels) caused by the vigorous motion of the alkyl chain above  $T_c$ .<sup>2-7)</sup> The DSC results showed that the motion of the alkyl chains of the  $\text{BF}_4^-$ -salts above  $T_c$  are less vigorous than those of the Br-salts. Therefore, the conduction channels of the  $\text{BF}_4^-$  are formed less effectively in the present materials than those of  $\text{Br}^-$  in  $C_n\text{-DABCO-}C_n\text{-Br}_2$ . Moreover,  $\text{BF}_4^-$  is a bigger anion than  $\text{Br}^-$ , and so the transport of  $\text{BF}_4^-$  is more retarded than that of  $\text{Br}^-$ . Accordingly, the ionic conductivities themselves of the  $\text{BF}_4^-$ -salts were lower than those of the Br-salts.<sup>14)</sup> All of these effects lead to the smaller values of  $\sigma_h/\sigma_l$  for the  $\text{BF}_4^-$ -salts than those for the Br-salts. No correlation was found between the  $\sigma_h/\sigma_l$  values of  $C_n\text{-DABCO-}C_n\text{-(BF}_4)_2$  ( $11 \leq n \leq 22$ ) and those of the corresponding  $C_n\text{-DABCO-}C_n\text{-Br}_2$  ( $11 \leq n \leq 22$ ). Comparing the ionic conductivities themselves,  $C_n\text{-DABCO-}C_n\text{-Br}_2$  showed almost identical values above  $T_c$ , irrespective of  $n$ ,<sup>2)</sup> although they were very different below  $T_c$ . On the other hand, the



(a)



(b)

Fig. 5. Disappearance of optical anisotropy of  $C_{14}\text{-DABCO-}C_{14}\text{-(BF}_4)_2$  observed by polarization microscope under a crossed Nicols condition.  
 (a) 60 °C, (b) 105 °C.

ionic conductivities of the present materials were very different below and above  $T_c$ . The reason for this remains to be clarified. The activation energies ( $\Delta E$ ) of the ionic conductivities were 0–13 and 16–94 kJ mol<sup>-1</sup> above and below  $T_c$  respectively.<sup>15</sup> The small  $\Delta E$  values of some of the materials above  $T_c$  suggest liquid-like anion transport in the solid.

**Observation by Polarization Microscope.** The IR absorption spectra of  $C_n$ -DABCO- $C_n$ -(BF<sub>4</sub>)<sub>2</sub> demonstrated a vigorous motion of the alkyl chain above  $T_c$ . The temperature dependence of the ionic conductivities of BF<sub>4</sub><sup>-</sup> suggested a liquid-like anion transport above  $T_c$ . These phenomena can be visualized by observing the sample crystal under a polarization microscope. Figure 5 shows photographs of C<sub>14</sub>-DABCO-C<sub>14</sub>-(BF<sub>4</sub>)<sub>2</sub> ( $T_c=96^\circ\text{C}$ ) under a crossed Nicols condition at 60 and 105 °C as examples. The crystal looked bright far below  $T_c$  as a result of optical anisotropy (Fig. 5(a)). When the temperature of the sample was elevated, the optical anisotropy began to diminish around 80 °C, and it disappeared completely around 100 °C without changing the crystal shape (Fig. 5(b)). These phenomena were not so sharp as in the case of Br-salts.<sup>16</sup> In these cases, the disappearance of the optical anisotropy of the crystal occurred very sharply (within 1 °C). The wide temperature range of the disappearance of the optical anisotropy suggests that the movement of the alkyl group already begins below  $T_c$  and that it becomes more vigorous as the temperature is elevated. Although a single and sharp DSC signal was observed at  $T_c$ , it does not justify the simple picture that the movement of the alkyl group begins suddenly at  $T_c$ .<sup>17</sup>

### Summary

The phase transitions of  $C_n$ -DABCO- $C_n$ -(BF<sub>4</sub>)<sub>2</sub> ( $10 \leq n \leq 22$ ) were studied by means of DSC, the IR absorption spectra, and measurements of the ionic conductivities of BF<sub>4</sub><sup>-</sup>. These materials exhibited conductivity jumps of BF<sub>4</sub><sup>-</sup>, as in the cases of  $C_n$ -DABCO- $C_n$ -X<sub>2</sub> (X=Cl, Br, I). The conductivity jumps were induced by the vigorous motion of the alkyl chain in the solid. A comparison of the conductivity jumps of BF<sub>4</sub>-salts with those of Br-salts showed that the former gave smaller values of  $\sigma_h/\sigma_l$  by one to two orders of magnitude. When the  $T_c$ ,  $\Delta H$ , and  $\Delta S$  values of BF<sub>4</sub>-salts were compared with those of the corresponding Br-salts, the former were found to give higher  $T_c$  and smaller  $\Delta H$  (and  $\Delta S$ ) than the latter. All of these experimental results led to the conclusions that BF<sub>4</sub>-salts are harder than the corresponding Br-salts in the low-temperature phase and that the motion of the alkyl chain of the former salts is less vigorous than that of the latter in the high-temperature phase.

We are grateful to Professor Shigekazu Kusabayashi and Dr. Shunsuke Takenaka, Faculty of Engineering,

Osaka University, for allowing us to use the DSC apparatus and the polarization microscope. The present work was supported by a Grant-in-Aid for Special Project Research on Chemical Sensors (No. 62217014) from the Ministry of Education, Science and Culture.

### References

- 1) J. Shimizu, T. Nogami, and H. Mikawa, *Solid State Commun.*, **54**, 1009 (1985).
- 2) J. Shimizu, K. Imamura, T. Nogami, and H. Mikawa, *Bull. Chem. Soc. Jpn.*, **59**, 1443 (1986).
- 3) K. Imamura, J. Shimizu, and T. Nogami, *Bull. Chem. Soc. Jpn.*, **59**, 2699 (1986).
- 4) J. Shimizu, K. Imamura, T. Nogami, and H. Mikawa, *Bull. Chem. Soc. Jpn.*, **59**, 3367 (1986).
- 5) K. Imamura, T. Nogami, and Y. Shiota, *Bull. Chem. Soc. Jpn.*, **60**, 111 (1987).
- 6) K. Imamura, T. Nogami, and Y. Shiota, *Bull. Chem. Soc. Jpn.*, **60**, 3499 (1987).
- 7) K. Imamura, T. Nogami, Y. Shiota, T. Ishioka, and M. Kobayashi, *Bull. Chem. Soc. Jpn.*, **60**, 3879 (1987).
- 8) The phase transition of DABCO has already been reported: T. Wada, E. Kishida, Y. Tomiie, H. Suga, S. Seki, and I. Nitta, *Bull. Chem. Soc. Jpn.*, **33**, 1317 (1960).
- 9) After the reaction, the methyl alcohol was evaporated to dryness and the residual solid was washed with hexane for  $1 \leq n \leq 5$  or with benzene for  $6 \leq n \leq 9$ , and then dried in a vacuum.
- 10) Analytical data (%) of  $C_n$ -DABCO- $C_n$ -(BF<sub>4</sub>)<sub>2</sub> (Found/Calcd).  
 $n=10$ : C, 54.52/54.95; H, 9.40/ 9.58; N, 4.84/4.93.  
 $n=11$ : C, 56.39/56.24; H, 9.82/ 9.80; N, 4.61/4.70.  
 $n=12$ : C, 57.74/57.70; H, 10.13/10.01; N, 4.49/4.49.  
 $n=13$ : C, 58.89/58.90; H, 10.26/10.19; N, 4.22/4.29.  
 $n=14$ : C, 59.80/60.01; H, 10.40/10.37; N, 4.01/4.12.  
 $n=15$ : C, 60.85/61.02; H, 10.57/10.53; N, 3.95/3.95.  
 $n=16$ : C, 61.88/61.96; H, 10.80/10.67; N, 3.74/3.80.  
 $n=17$ : C, 62.74/62.83; H, 10.81/10.81; N, 3.65/3.66.  
 $n=18$ : C, 63.31/63.63; H, 10.90/10.93; N, 3.51/3.53.  
 $n=22$ : C, 65.76/66.36; H, 11.25/11.36; N, 3.02/3.10.
- 11) Since the samples were dried around 80 °C in a vacuum overnight before the measurements, the effect of the moisture on the ionic conductivity can be neglected.
- 12) The conductivity jumps were found to occur within the following temperature widths: 1.7 °C ( $n=11$ ), 3.7 °C ( $n=12$ ), 2.7 °C ( $n=13$ ), 2.5 °C ( $n=14$ ), 2.3 °C ( $n=15$ ), 2.5 °C ( $n=16$ ), 4.5 °C ( $n=17$ ), 5.7 °C ( $n=18$ ), 3.5 °C ( $n=22$ ).
- 13) The transition temperatures of  $C_n$ -DABCO- $C_n$ -(BF<sub>4</sub>)<sub>2</sub>, obtained by the use of the mid-points of the conductivity jumps, are as follows (they are close to those obtained by DSC (cf. Table 2)): 80 °C ( $n=11$ ), 92 °C ( $n=12$ ), 93 °C ( $n=13$ ), 96 °C ( $n=14$ ), 100 °C ( $n=15$ ), 101 °C ( $n=16$ ), 101 °C ( $n=17$ ), 101 °C ( $n=18$ ), 109 °C ( $n=22$ ).
- 14) The ionic conductivities of BF<sub>4</sub>-salts above  $T_c$  were by one to two orders of magnitude smaller than those of the Br-salts (cf. Ref. 2).
- 15) The activation energies ( $\Delta E$ ) of the ionic conductivities of  $C_n$ -DABCO- $C_n$ -(BF<sub>4</sub>)<sub>2</sub> are as follows (kJ mol<sup>-1</sup>) (with the ranges of the temperature (°C) for the calculation of  $\Delta E$  in the low-temperature phase shown in parentheses): Below

$T_c$ : 55 ( $n=11$ ,  $67 \leq T \leq 79$ ), 68 ( $n=12$ ,  $74 \leq T \leq 91$ ), 56 ( $n=13$ ,  $79 \leq T \leq 89$ ), 20 ( $n=14$ ,  $85 \leq T \leq 97$ ), 32 ( $n=15$ ,  $79 \leq T \leq 98$ ), 16 ( $n=16$ ,  $90 \leq T \leq 102$ ), 94 ( $n=17$ ,  $87 \leq T \leq 98$ ), 17 ( $n=18$ ,  $85 \leq T \leq 99$ ), 65 ( $n=22$ ,  $88 \leq T \leq 107$ ). Above  $T_c$ : 5 ( $n=11$ ), 3 ( $n=12$ ), 7 ( $n=13$ ), 7 ( $n=14$ ), 0 ( $n=15$ ), 7 ( $n=16$ ), 4 ( $n=17$ ), 3 ( $n=18$ ), 13 ( $n=22$ ). The activation energies below the lower limit of the temperature shown in the parentheses are much smaller than those calculated especially for  $n=15$ , 16, 17, 18,

and 22. The reasons for this remain to be clarified.

16) T. Nogami, *Kagaku*, **43**, 169 (1988).

17) Detailed measurements of the  $^1\text{H}$  spin-lattice relaxation time of  $\text{C}_{10}\text{-DABCO-C}_{10}\text{-X}_2$  ( $\text{X}=\text{Br}$ ,  $\text{I}$ ) demonstrated that the movement of the alkyl chain also begins below  $T_c$ . H. Nakayama, T. Eguchi, N. Nakamura, H. Chihara, T. Nogami, K. Imamura, and Y. Shirota, *Bull. Chem. Soc. Jpn.*, in press.

---